

Probing Strangeness Hadronization with Event-by-Event Production of Multistrange Hadrons

Original

Probing Strangeness Hadronization with Event-by-Event Production of Multistrange Hadrons / Acharya, S., Adamová, D., Agarwal, A., Aglieri Rinella, G., Aglietta, L., Agnello, M., Agrawal, N., Ahammed, Z., Ahmad, S., Ahn, S.u., Ahuja, I., Akindinov, A., Akishina, V., Al-Turany, M., Aleksandrov, D., Alessandro, B., Alfanda, H.m., Alfaro Molina, R., Ali, B., Alici, A., et al.. - In: PHYSICAL REVIEW LETTERS. - ISSN 0031-9007. - STAMPA. - 134:2(2025).
[10.1103/physrevlett.134.022303]

Availability:

This version is available at: 11583/3001053 since: 2025-06-17T20:50:12Z

Publisher:

American Physical Society

Published

DOI:10.1103/physrevlett.134.022303

Terms of use:

This article is made available under terms and conditions as specified in the corresponding bibliographic description in the repository

Publisher copyright

(Article begins on next page)

Probing Strangeness Hadronization with Event-by-Event Production of Multistrange Hadrons

S. Acharya *et al.**
(ALICE Collaboration)

 (Received 22 July 2024; accepted 5 November 2024; published 17 January 2025)

This Letter presents the first measurement of event-by-event fluctuations of the net number (difference between the particle and antiparticle multiplicities) of multistrange hadrons Ξ^- and Ξ^+ and its correlation with the net-kaon number using the data collected by the ALICE Collaboration in pp, p-Pb, and Pb-Pb collisions at a center-of-mass energy per nucleon pair $\sqrt{s_{NN}} = 5.02$ TeV. The statistical hadronization model with a correlation over three units of rapidity between hadrons having the same and opposite strangeness content successfully describes the results. On the other hand, string-fragmentation models that mainly correlate strange hadrons with opposite strange quark content over a small rapidity range fail to describe the data.

DOI: [10.1103/PhysRevLett.134.022303](https://doi.org/10.1103/PhysRevLett.134.022303)

In high-energy hadronic and heavy-ion collisions, strange quarks are dominantly produced from gluon fusion [1]. In Pb–Pb collisions at the Large Hadron Collider (LHC), a thermalized medium of deconfined partons, the strongly-interacting quark–gluon plasma (sQGP) is expected to form, where the efficient production of strange–antistrange quark pairs enables the thermal and chemical equilibration of strangeness in the medium [1,2]. Various experimental results from high-multiplicity p. p. collisions at the LHC demonstrate striking similarities to results from Pb–Pb collisions. Notably, the ratios between strange and nonstrange hadron yields show a smooth increase with increasing particle multiplicity across collision systems [3–5], and the patterns of multiparticle correlations in p. p. collisions closely resemble those seen in Pb–Pb collisions [6–9]. Theoretically, explaining such experimental observations, and the hadron production in general, requires phenomenological modeling of the hadronization process, as its inherently nonperturbative nature prevents us from performing reliable quantum chromodynamics (QCD) *ab initio* calculations. Two different approaches, namely statistical hadronization [10,11] and Lund string fragmentation [12], are commonly employed to address this problem. The statistical hadronization model (SHM) is based on a thermodynamic approach and the hadron abundances are determined at the freeze-out of inelastic interactions from the derivatives of the partition

function of the system, which is assumed to be an ideal gas of hadrons and resonances (HRG) at local equilibrium. Event-by-event conservation laws are implemented using the canonical ensemble (CE) formulation of statistical mechanics [13,14]. Using the CE, the SHM model can describe the yield of light-flavored particles across all colliding systems with a precision better than 20% [15,16]. The SHM implementations of Refs. [15,16] differ in the parametrizations of the system volume, V , and chemical freeze-out temperature, T_{chem} , as well as in the accounting for a possible incomplete thermalization of the total strangeness at low multiplicity via a strangeness saturation factor, γ_s [17]. On the other hand, in the string-fragmentation picture, as implemented in PYTHIA [18], final-state partons are connected by color flux tubes, known as strings, which break up into smaller segments for large string lengths. Additional quark–antiquark pairs are produced during this process: once no more energy is available for further splitting, hadrons are formed. The starting string configuration for hadronization is determined by the arrangement of opposite colors and anticolors according to color reconnection mechanisms [18–20]. Adding further interactions between the strings leading to the formation of baryon junctions [20] and ropes [21], PYTHIA can describe the multiplicity dependence of the ratio between the yields of strange and nonstrange particles [22]. Consequently, new observables are needed to discriminate between these two approaches.

String fragmentation and canonical statistical hadronization provide different treatments of the conservation laws. In the former, quantum numbers are conserved at a local level because of the formation of quark–antiquark pairs in the string breaking process, while in the latter, conservation laws hold over a finite correlation volume, V_c [15].

*Full author list given at the end of the Letter.

Published by the American Physical Society under the terms of the [Creative Commons Attribution 4.0 International license](https://creativecommons.org/licenses/by/4.0/). Further distribution of this work must maintain attribution to the author(s) and the published article's title, journal citation, and DOI. Open access publication funded by CERN.

Consequently, canonical charge conservation implies correlations between any two hadrons carrying either same- or opposite-sign quantum numbers, showing a decreasing correlation strength for increasing correlation volume. Instead, in the string fragmentation model, a strong correlation exists mostly between oppositely-charged hadrons because of the quantum number conservation at each string breaking. In principle, such an effect has no significant multiplicity dependence, except from that coming from specific implementations of the color reconnection mechanism.

The difference in the quantum number conservation between these two models can be probed by analyzing the event-by-event correlation between different hadron species. This approach has previously been applied by the ALICE Collaboration to study baryon number conservation via net-proton fluctuations [23]. There, it was concluded that baryon number is conserved through long rapidity-range correlations. In this Letter, the first study in this regard in the strangeness sector is presented analyzing the event-by-event correlation between charged kaons and Ξ^- and Ξ^+ baryons. In the following, Ξ is used instead of Ξ^- and Ξ^+ for brevity, unless otherwise specified. These species are chosen because they are minimally affected by correlations other than those induced by the quantum number conservation, e.g. by the decay of heavier states into charged kaons and Ξ baryons. In addition, their production is only marginally affected by weak feed down, which comes from Ω -baryon decays. The observables considered in this Letter are the normalized second-order cumulant of net- Ξ number and the correlation between net- Ξ and net-kaon numbers. The net-particle numbers are defined in terms of the event-by-event multiplicities, n , of particles and antiparticles as $n_{\Delta K} = n_{K^+} - n_{K^-}$ and $n_{\Delta \Xi} = n_{\Xi^+} - n_{\Xi^-}$ for charged kaons and charged Ξ baryons, respectively. The normalized second-order cumulant of net- Ξ number and the correlation between net- Ξ and net-kaon numbers are defined as

$$\frac{\kappa_2(\Delta \Xi)}{\kappa_1(\Xi^+ + \Xi^-)} = \frac{\kappa_2(\Xi^+) + \kappa_2(\Xi^-) - 2\kappa_{11}(\Xi^+, \Xi^-)}{\kappa_1(\Xi^+ + \Xi^-)}, \quad (1)$$

$$\rho_{\Delta \Xi \Delta K} = \frac{\kappa_{11}(\Xi^+, K^+) + \kappa_{11}(\Xi^-, K^-) - \kappa_{11}(\Xi^+, K^-) - \kappa_{11}(\Xi^-, K^+)}{\sqrt{\kappa_2(\Delta \Xi) \kappa_2(\Delta K)}}, \quad (2)$$

respectively, where

$$\kappa_1(A) = \langle n_A \rangle, \quad (3)$$

$$\kappa_2(A) = \langle n_A^2 \rangle - \langle n_A \rangle^2, \quad (4)$$

$$\kappa_{11}(A, B) = \langle n_A n_B \rangle - \langle n_A \rangle \langle n_B \rangle, \quad (5)$$

and $n_{A,B}$ and $\langle n_{A,B} \rangle$ indicate the event-by-event and event-averaged number of particles of species A or B, respectively. The m th order cumulants of net particles are denoted as κ_m in Eqs. (1) and (2). The normalized second-order cumulant is only affected by opposite strangeness sign correlation, whereas both the correlations of same- and opposite-strangeness pairs have an impact on $\rho_{\Delta \Xi \Delta K}$. Both observables are sensitive to the locality of strangeness conservation, which affects the magnitude of the correlations. Therefore, these observables are powerful tools to distinguish among different hadronization scenarios. In addition, the studied quantities are independent of volume fluctuations under the hypothesis of particle-antiparticle balance at the energies available at the LHC from small to large systems [24,25].

The results reported in this Letter are extracted from data collected by the ALICE Collaboration in p. p., p-Pb, and Pb-Pb collisions at a center-of-mass energy per nucleon-nucleon pair $\sqrt{s_{NN}} = 5.02$ TeV. The ALICE apparatus and its performance are described in detail in Refs. [26,27]. Events are selected with a minimum bias (MB) trigger based on a coincidence of signals in the two V0 scintillator arrays [28], which are placed at both sides of the nominal interaction point, covering the pseudorapidity, η , intervals $-3.7 < \eta < -1.7$ and $2.8 < \eta < 5.1$. In the Pb-Pb sample, an additional trigger based on the amplitude of the V0 signal is applied to enhance the selection of central (head-on) and semicentral collisions. Further selections are applied to reject pileup events [29]. Finally, the position of the reconstructed primary vertex (PV) along the beam direction (z axis) is required to be within 10 cm around the nominal interaction point. After event selections, the datasets consist of about 900×10^6 p.p. collisions, 600×10^6 p-Pb collisions, and 400×10^6 Pb-Pb collisions. The selected samples are subdivided into multiplicity classes defined according to the signal amplitudes measured in the V0 detectors [30].

Charged particles are tracked in the central-barrel detectors of ALICE, which cover the full azimuth in the midrapidity region. The pseudorapidity acceptance of the present measurement is $|\eta| < 0.8$. The charged kaon and charged Ξ candidates are selected in the transverse momentum (p_T) ranges $0.2 < p_T < 1.0$ GeV/ c and $1.0 < p_T < 3.0$ GeV/ c , respectively, to cover the bulk of the production. The purity of the selected samples of candidates in these momentum intervals is $\gtrsim 95\%$. Charged kaons are directly tracked in the detectors, while Ξ baryons are reconstructed via their weak decay to a charged pion and a Λ baryon: the latter is identified via its weak decay into a proton and a charged pion, $\Xi^- \rightarrow \pi^- + \Lambda (\rightarrow p + \pi^-)$. The charge-conjugate decay is employed for Ξ^+ .

The reconstruction of tracks is based on the space points measured in the inner tracking system (ITS) [31] and the time projection chamber (TPC) [32]. Track selections are

applied to ensure a good quality of the track reconstruction [33,34]. To avoid intersections in the samples of tracks used for the reconstruction of kaons and Ξ , which might produce spurious correlations, complementary selections are applied to the distance of closest approach (DCA) of tracks to the PV. Specifically, $|DCA| < 0.1$ cm for kaons, while $|DCA| > 0.1$ cm for Ξ -decay products. Tracked particles are identified by measuring their specific energy loss, dE/dx , in the TPC gas volume. For all candidates, the difference between the measured TPC dE/dx signal and the one expected for the considered particle species is required to be less than 3σ , where σ is the resolution on the dE/dx in the data assuming a Gaussian shape for the TPC particle identification (PID) signal. For kaons, additional particle selection criteria are applied: for candidates with $p_T < 0.4$ GeV/c in Pb-Pb collisions, the dE/dx measured with the ITS is used to improve the rejection of electrons and positrons; for $p_T > 0.4$ GeV/c, the particle velocity measured with the time-of-flight (TOF) detector is employed to reject charged pions and muons: the discrepancy between the measured velocity and the one expected for kaons is requested to be smaller than 3σ . The algorithm used to reconstruct the Ξ -decay vertices from tracks is similar to that used in previous studies [35–37]. A large fraction of combinatorial background contaminates the sample of selected Ξ candidates. To address this, a machine learning (ML) method is used to enhance the signal-over-background ratio of the sample, as detailed in Ref. [38]. The training of the ML algorithm is based on the cascade and two-body decay topological variables of the Ξ and Λ candidates, respectively. A few examples of the invariant-mass distribution of the selected Ξ and of the TPC and TOF PID variables of the selected kaons are reported in Ref. [38]. In the 10% most central Pb-Pb collisions, the average number of selected $\Xi^+ + \Xi^-$ and $K^+ + K^-$ is about 0.07 and 16 per collision, respectively, before applying efficiency corrections.

The observables defined in Eqs. (1) and (2) are corrected for the candidate-selection efficiency assuming a detector response with binomial fluctuations. The analytic expression for the efficiency correction of first- and second-order cumulants were obtained in previous works [39]. The efficiencies are calculated using MC simulations in which particles produced by an event generator (PYTHIA8 with Monash tune [18,19] for pp, EPOS LHC [40] for p-Pb, and HIJING [41] for Pb-Pb) are transported through an accurate model of the ALICE apparatus via GEANT4 [42]. The efficiencies are p_T and multiplicity dependent, ranging from 1% to 8% for Ξ baryons and from 5% to 30% for kaons. The resulting correction factors on $\rho_{\Delta\Xi\Delta K}$ and $\kappa_2(\Delta\Xi)/\kappa_1(\Xi^+ + \Xi^-)$ are 10 to 15 and 0.95, respectively. Using a closure test based on MC simulations, it was checked that the efficiency-correction procedure does not introduce any significant bias in the corrected cumulants.

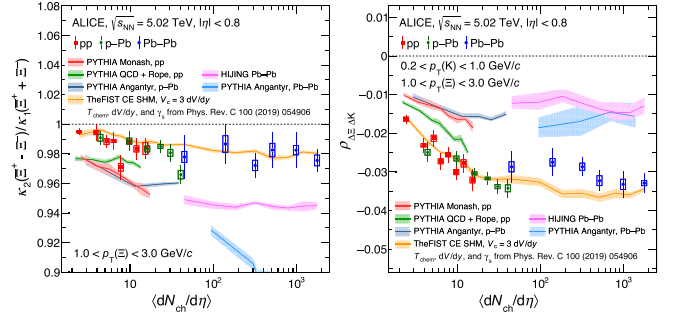


FIG. 1. Normalized second order cumulant of net Ξ (left panel) and correlation between net Ξ and net kaon (right panel), as a function of the average multiplicity at midrapidity, in p. p. (red squares), p-Pb (green diamonds), and Pb-Pb collisions (blue circles) at $\sqrt{s_{NN}} = 5.02$ TeV. Statistical and systematic uncertainties are shown via error bars and boxes, respectively. The experimental measurements are compared to several model predictions, shown as bands. The width of the bands represents the statistical uncertainty of the predictions. The average multiplicity values are obtained from Refs. [33,44,45]; their uncertainties are not shown in the plot.

The statistical uncertainties are estimated using the subsample method [43]. The systematic uncertainties are obtained by extracting cumulants and correlations using different variations of the candidate selection criteria. This procedure is repeated using several combinations of the different variations [38]. The systematic uncertainty associated to each of the sources are reported in Appendix A.1. The total systematic uncertainty in the cumulants is computed, for each multiplicity class, as the standard deviation of the results obtained with the different combinations. The average of the multitrial results is employed as the central value of the observable. The systematic uncertainties are fully correlated across different multiplicity intervals.

The normalized second-order cumulant of net Ξ and the correlation between net-kaon and net- Ξ numbers are shown in the left and right panels of Fig. 1, respectively. The observables are shown as a function of the average charged-particle multiplicity at midrapidity, $\langle dN_{ch}/d\eta \rangle$, enabling the comparison of the results from different colliding systems. The results show a continuous evolution as a function of the multiplicity from pp to Pb-Pb collisions for the correlation term and the normalized second-order cumulant. The measurements are compared to the SHM and Lund string-fragmentation model, to probe the correlation volume between strange hadrons and the presence of same-sign correlations originating from the different treatments of net-strangeness conservation. The width of the bands in Fig. 1 depicts the statistical uncertainty of the MC simulations corresponding to the different models. A long-range rapidity correlation implies a smaller deviation from the Poisson baseline, corresponding to the grand canonical ensemble (GCE) limit, than a short-range correlation,

which is generally present in string models. For the normalized second-order cumulant of net Ξ , the Poisson baseline equals unity, while it is zero for $\rho_{\Delta\Xi\Delta K}$. The predictions of the SHM within the CE framework, shown in Fig. 1, are obtained with the Thermal-FIST package [46]. The model parameters, such as the chemical freeze-out temperature, T_{chem} , and the volume per unit of rapidity, dV/dy , are tuned using the hadron yields measured by ALICE and setting the correlation volume to $V_c = 3dV/dy$. The model includes a strangeness saturation parameter, γ_s , which accounts for incomplete total strangeness equilibration at $\langle dN_{\text{ch}}/d\eta \rangle \lesssim 100$ [15]. This parameter is needed in Thermal-FIST to describe the average yields of (multi)strange hadrons but it does not have any significant effect on the observables shown in Fig. 1. This parametrization allows us to describe both the normalized second-order cumulant of net Ξ and $\rho_{\Delta\Xi\Delta K}$ within uncertainties, with a slight tension in semicentral Pb-Pb collisions for $\rho_{\Delta\Xi\Delta K}$. Predictions from the Lund string-fragmentation models for the high-multiplicity regime corresponding to heavy-ion collisions are obtained with HIJING [41] and PYTHIA Angantyr [47]. The Angantyr model is also used for p-Pb collisions, while for p. p. collisions, the PYTHIA model with different color reconnection (CR) schemes is used [18]. The predictions shown in Fig. 1 are obtained either with the multiparton-interaction (MPI) based CR (Monash tune [19]) or with a QCD-based CR approach [20]. For the latter calculation, the effect of rope hadronization, in which spatially overlapping strings are allowed to combine into ropes with a larger effective string tension, is also included. Rope hadronization is responsible for an enhancement in the production of strangeness [20], while the QCD CR describes an increase in baryon production due to the formation of baryon junctions [21].

The normalized second-order cumulants of net Ξ are consistently below unity over the entire multiplicity range, which can be understood as an effect of quantum number (baryon, strangeness) conservation [48]. The results are consistent with the SHM with a correlation range of three units of rapidity throughout the analyzed collision systems. In the context of the SHM, this suggests the presence of a long-range rapidity correlation between two hadrons with opposite strangeness contents due to the conservation of strangeness. On the other hand the different kinds of string models overestimate the strength of the correlation, which is quantified by the deviation of the predictions from unity.

Furthermore, the measured correlation between net kaon and net Ξ , $\rho_{\Delta\Xi\Delta K}$, is sensitive to the range of the correlation due to strangeness conservation and to the possible correlation between hadrons with same-sign strange quantum numbers. A significant anticorrelation between net kaon and net- Ξ is observed across all collision systems. Even though the string fragmentation model has small-range rapidity correlation, the SHM predicts a more significant deviation from the Poisson baseline with respect

to the string fragmentation model, as the latter does not include any significant correlations among hadrons with same-sign strangeness. The SHM prediction describes the measured $\rho_{\Delta\Xi\Delta K}$, indicating a sizeable contribution of same strangeness sign correlation.

From the simultaneous fit of the $\rho_{\Delta\Xi\Delta K}$ and normalized second-order cumulant for net Ξ in Pb-Pb collisions using the Thermal-FIST package, the correlation volume is determined to be $V_c = 3.19 \pm 0.14 dV/dy$, with a fit probability of $P = 0.94$ (see Appendix A.2 for further details). This volume, valid only for Pb-Pb collisions, is compatible within 1.4σ with a value $V_c = 3 dV/dy$, which was obtained in previous analyses of hadron yield ratios within the canonical statistical model across different colliding systems [15]. In the context of the SHM, this result shows that a large correlation volume regulates the conservation of strangeness, implying that correlations are formed at earlier times than predicted by string fragmentation. A large correlation volume for baryon number conservation was also observed from the study of net-proton fluctuations. See a comparison between the experimental data from the ALICE Collaboration and the predictions obtained with Thermal-FIST in Appendix A.3. On the other hand, a correlation volume of $1.6 dV/dy$ was obtained from the analysis of event-by-event fluctuations of anti-deuterons [49], possibly because the formation of bound objects such as light nuclei differs from the production of other light-flavor hadrons. Specifically, these results might indicate later formation times of light nuclei compared to other hadron species [50].

In summary, the simultaneous measurement of both the presented observables has a high discriminative power against the different model predictions. The correlation and normalized second-order cumulant measurements are well described by the CE SHM formalism. The model reproduces both the absolute value of the observables and their multiplicity trends. These results are consistent with previous work [15], in which the yield ratios of charged particles, such as Ξ/π , in pp, p-Pb, and Pb-Pb collisions were also studied within the framework of the canonical statistical model implemented in Thermal-FIST. All of the tested predictions based on nonthermally equilibrated systems and string fragmentation, qualitatively describe a negative correlation of net- Ξ and net-kaon numbers, along with a normalized second-order cumulant smaller than one. However, they fail to quantitatively describe the experimental results, both in the low- and high-multiplicity regions. The PYTHIA8 tune closest to the experimental results is the QCD-based CR approach with rope hadronization: this model can describe the hadron yield ratios at low multiplicity, as shown in previous studies [22]. Nevertheless, a significant combined deviation of 7.5σ between the data in p.p. collisions and the string fragmentation predictions is observed. Such a discrepancy could be

resolved only by simultaneously including long-range and same-sign correlations in the string fragmentation framework. Such long-range correlations are a feature of the thermally-equilibrated system modeled by Thermal-FIST that successfully describe the measurements. It is possible that for cumulants higher than the second order, deviations from the thermal baseline might occur, as these are associated with different relaxation times to reach thermalization [51] or due to the presence of a phase transition [52]. Such a scenario could be probed in the future, with the ongoing LHC Run 3 data, extending such studies to higher order cumulants. Furthermore, the measurements provided here can also be used to probe the correlation volume in more elaborated statistical hadronization models such as in Ref. [53].

Acknowledgments—The ALICE Collaboration would like to thank all its engineers and technicians for their invaluable contributions to the construction of the experiment and the CERN accelerator teams for the outstanding performance of the LHC complex. The ALICE Collaboration gratefully acknowledges the resources and support provided by all Grid centres and the Worldwide LHC Computing Grid (WLCG) collaboration. The ALICE Collaboration acknowledges the following funding agencies for their support in building and running the ALICE detector: A. I. Alikhanyan National Science Laboratory (Yerevan Physics Institute) Foundation (ANSL), State Committee of Science and World Federation of Scientists (WFS), Armenia; Austrian Academy of Sciences, Austrian Science Fund (FWF): [M 2467-N36] and Nationalstiftung für Forschung, Technologie und Entwicklung, Austria; Ministry of Communications and High Technologies, National Nuclear Research Center, Azerbaijan; Conselho Nacional de Desenvolvimento Científico e Tecnológico (CNPq), Financiadora de Estudos e Projetos (Finep), Fundação de Amparo à Pesquisa do Estado de São Paulo (FAPESP) and Universidade Federal do Rio Grande do Sul (UFRGS), Brazil; Bulgarian Ministry of Education and Science, within the National Roadmap for Research Infrastructures 2020–2027 (object CERN), Bulgaria; Ministry of Education of China (MOEC), Ministry of Science & Technology of China (MSTC) and National Natural Science Foundation of China (NSFC), China; Ministry of Science and Education and Croatian Science Foundation, Croatia; Centro de Aplicaciones Tecnológicas y Desarrollo Nuclear (CEADEN), Cubaenergía, Cuba; Ministry of Education, Youth and Sports of the Czech Republic, Czech Republic; The Danish Council for Independent Research | Natural Sciences, the VILLUM FONDEN and Danish National Research Foundation (DNRF), Denmark; Helsinki Institute of Physics (HIP), Finland; Commissariat à l’Energie Atomique (CEA) and

Institut National de Physique Nucléaire et de Physique des Particules (IN2P3) and Centre National de la Recherche Scientifique (CNRS), France; Bundesministerium für Bildung und Forschung (BMBF) and GSI Helmholtzzentrum für Schwerionenforschung GmbH, Germany; General Secretariat for Research and Technology, Ministry of Education, Research and Religions, Greece; National Research, Development and Innovation Office, Hungary; Department of Atomic Energy Government of India (DAE), Department of Science and Technology, Government of India (DST), University Grants Commission, Government of India (UGC) and Council of Scientific and Industrial Research (CSIR), India; National Research and Innovation Agency–BRIN, Indonesia; Istituto Nazionale di Fisica Nucleare (INFN), Italy; Japanese Ministry of Education, Culture, Sports, Science and Technology (MEXT) and Japan Society for the Promotion of Science (JSPS) KAKENHI, Japan; Consejo Nacional de Ciencia (CONACYT) y Tecnología, through Fondo de Cooperación Internacional en Ciencia y Tecnología (FONCICYT) and Dirección General de Asuntos del Personal Académico (DGAPA), Mexico; Nederlandse Organisatie voor Wetenschappelijk Onderzoek (NWO), Netherlands; The Research Council of Norway, Norway; Pontificia Universidad Católica del Perú, Peru; Ministry of Science and Higher Education, National Science Centre and WUT ID-UB, Poland; Korea Institute of Science and Technology Information and National Research Foundation of Korea (NRF), Republic of Korea; Ministry of Education and Scientific Research, Institute of Atomic Physics, Ministry of Research and Innovation and Institute of Atomic Physics and Universitatea Nationala de Stiinta si Tehnologie Politehnica Bucuresti, Romania; Ministry of Education, Science, Research and Sport of the Slovak Republic, Slovakia; National Research Foundation of South Africa, South Africa; Swedish Research Council (VR) and Knut & Alice Wallenberg Foundation (KAW), Sweden; European Organization for Nuclear Research, Switzerland; Suranaree University of Technology (SUT), National Science and Technology Development Agency (NSTDA) and National Science, Research and Innovation Fund (NSRF via PMU-B B05F650021), Thailand; Turkish Energy, Nuclear and Mineral Research Agency (TENMAK), Turkey; National Academy of Sciences of Ukraine, Ukraine; Science and Technology Facilities Council (STFC), United Kingdom; National Science Foundation of the United States of America (NSF) and United States Department of Energy, Office of Nuclear Physics (DOE NP), United States of America. In addition, individual groups or members have received support from: Czech Science Foundation (Grant No. 23-07499S), Czech Republic; European Research Council (Grant No. 950692), European Union; ICSC–Centro Nazionale di Ricerca in High Performance

Computing, Big Data and Quantum Computing, European Union—NextGenerationEU; Academy of Finland (Center of Excellence in Quark Matter) (Grants No. 346327, No. 346328), Finland.

-
- [1] J. Rafelski and B. Muller, Strangeness production in the quark—gluon plasma, *Phys. Rev. Lett.* **48**, 1066 (1982); **56**, 2334(E) (1986).
- [2] P. Koch, B. Muller, and J. Rafelski, Strangeness in relativistic heavy ion collisions, *Phys. Rep.* **142**, 167 (1986).
- [3] J. Adam *et al.* (ALICE Collaboration), Enhanced production of multi-strange hadrons in high-multiplicity proton-proton collisions, *Nat. Phys.* **13**, 535 (2017).
- [4] S. Acharya *et al.* (ALICE Collaboration), Multiplicity dependence of light-flavor hadron production in pp collisions at $\sqrt{s} = 7$ TeV, *Phys. Rev. C* **99**, 024906 (2019).
- [5] S. Acharya *et al.* (ALICE Collaboration), Multiplicity dependence of (multi-)strange hadron production in proton-proton collisions at $\sqrt{s} = 13$ TeV, *Eur. Phys. J. C* **80**, 167 (2020).
- [6] B. Abelev *et al.* (ALICE Collaboration), Long-range angular correlations on the near and away side in p–Pb collisions at $\sqrt{s_{NN}} = 5.02$ TeV, *Phys. Lett. B* **719**, 29 (2013).
- [7] V. Khachatryan *et al.* (CMS Collaboration), Evidence for collectivity in pp collisions at the LHC, *Phys. Lett. B* **765**, 193 (2017).
- [8] S. Acharya *et al.* (ALICE Collaboration), Investigations of anisotropic flow using multiparticle azimuthal correlations in pp, p–Pb, Xe–Xe, and Pb–Pb collisions at the LHC, *Phys. Rev. Lett.* **123**, 142301 (2019).
- [9] S. Acharya *et al.* (ALICE Collaboration), Emergence of long-range angular correlations in low-multiplicity proton-proton collisions, *Phys. Rev. Lett.* **132**, 172302 (2024).
- [10] R. Hagedorn and J. Rafelski, Hot hadronic matter and nuclear collisions, *Phys. Lett.* **97B**, 136 (1980).
- [11] R. Hagedorn and K. Redlich, Statistical thermodynamics in relativistic particle and ion physics: Canonical or grand canonical?, *Z. Phys. C* **27**, 541 (1985).
- [12] B. Andersson, G. Gustafson, G. Ingelman, and T. Sjostrand, Parton fragmentation and string dynamics, *Phys. Rep.* **97**, 31 (1983).
- [13] A. Bzdak, V. Koch, and V. Skokov, Baryon number conservation and the cumulants of the net proton distribution, *Phys. Rev. C* **87**, 014901 (2013).
- [14] P. Braun-Munzinger, B. Friman, K. Redlich, A. Rustamov, and J. Stachel, Relativistic nuclear collisions: Establishing a non-critical baseline for fluctuation measurements, *Nucl. Phys. A* **1008**, 122141 (2021).
- [15] V. Vovchenko, B. Dönigus, and H. Stoecker, Canonical statistical model analysis of p–p, p–Pb, and Pb–Pb collisions at energies available at the CERN Large Hadron Collider, *Phys. Rev. C* **100**, 054906 (2019).
- [16] J. Cleymans, P.M. Lo, K. Redlich, and N. Sharma, Multiplicity dependence of (multi)strange baryons in the canonical ensemble with phase shift corrections, *Phys. Rev. C* **103**, 014904 (2021).
- [17] J. Letessier, A. Tounsi, U. W. Heinz, J. Sollfrank, and J. Rafelski, Strangeness conservation in hot nuclear fireballs, *Phys. Rev. D* **51**, 3408 (1995).
- [18] C. Bierlich *et al.*, A comprehensive guide to the physics and usage of PYTHIA8.3, *SciPost Phys. Codebases* **2022**, 8 (2022).
- [19] P. Skands, S. Carrazza, and J. Rojo, Tuning PYTHIA8.1: The Monash 2013 tune, *Eur. Phys. J. C* **74**, 3024 (2014).
- [20] J. Christiansen and P. Skands, String formation beyond leading colour, *J. High Energy Phys.* **08** (2015) 003.
- [21] C. Bierlich, G. Gustafson, L. Lönnblad, and A. Tarasov, Effects of overlapping strings in pp collisions, *J. High Energy Phys.* **03** (2015) 148.
- [22] R. Nayak, S. Pal, and S. Dash, Effect of rope hadronization on strangeness enhancement in p–p collisions at LHC energies, *Phys. Rev. D* **100**, 074023 (2019).
- [23] S. Acharya *et al.* (ALICE Collaboration), Global baryon number conservation encoded in net-proton fluctuations measured in Pb–Pb collisions at $\sqrt{s_{NN}} = 2.76$ TeV, *Phys. Lett. B* **807**, 135564 (2020).
- [24] P. Braun-Munzinger, A. Rustamov, and J. Stachel, Bridging the gap between event-by-event fluctuation measurements and theory predictions in relativistic nuclear collisions, *Nucl. Phys. A* **960**, 114 (2017).
- [25] S. Acharya *et al.* (ALICE Collaboration), Measurements of chemical potentials in Pb–Pb collisions at $\sqrt{s_{NN}} = 5.02$ TeV, *Phys. Rev. Lett.* **133**, 092301 (2024).
- [26] K. Aamodt *et al.* (ALICE Collaboration), The ALICE experiment at the CERN LHC, *J. Instrum.* **3**, S08002 (2008).
- [27] B. Abelev *et al.* (ALICE Collaboration), Performance of the ALICE experiment at the CERN LHC, *Int. J. Mod. Phys. A* **29**, 1430044 (2014).
- [28] E. Abbas *et al.* (ALICE Collaboration), Performance of the ALICE VZERO system, *J. Instrum.* **8**, P10016 (2013).
- [29] M. Arslanodk, E. Hellbär, M. Ivanov, R. H. Münzer, and J. Wiechula, Track reconstruction in a high-density environment with ALICE, *Particles* **5**, 84 (2022).
- [30] ALICE Collaboration, Centrality determination in heavy ion collisions, Report No. ALICE-PUBLIC-2018-011, CERN, 2018, <https://cds.cern.ch/record/2636623>.
- [31] K. Aamodt *et al.* (ALICE Collaboration), Alignment of the ALICE inner tracking system with cosmic-ray tracks, *J. Instrum.* **5**, P03003 (2010).
- [32] J. Alme *et al.*, The ALICE TPC, a large 3-dimensional tracking device with fast readout for ultra-high multiplicity events, *Nucl. Instrum. Methods Phys. Res., Sect. A* **622**, 316 (2010).
- [33] B. Abelev *et al.* (ALICE Collaboration), Multiplicity dependence of pion, kaon, proton and lambda production in p–Pb collisions at $\sqrt{s_{NN}} = 5.02$ TeV, *Phys. Lett. B* **728**, 25 (2014).
- [34] S. Acharya *et al.* (ALICE Collaboration), Production of charged pions, kaons, and (anti-)protons in Pb–Pb and inelastic pp collisions at $\sqrt{s_{NN}} = 5.02$ TeV, *Phys. Rev. C* **101**, 044907 (2020).
- [35] B. Abelev *et al.* (ALICE Collaboration), Multi-strange baryon production in pp collisions at $\sqrt{s} = 7$ TeV with ALICE, *Phys. Lett. B* **712**, 309 (2012).
- [36] B. Abelev *et al.* (ALICE Collaboration), Multi-strange baryon production at mid-rapidity in Pb–Pb collisions at $\sqrt{s_{NN}} = 2.76$ TeV, *Phys. Lett. B* **728**, 216 (2014); **734**, 409(E) (2014).

- [37] J. Adam *et al.* (ALICE Collaboration), Multi-strange baryon production in p–Pb collisions at $\sqrt{s_{NN}} = 5.02$ TeV, *Phys. Lett. B* **758**, 389 (2016).
- [38] ALICE Collaboration, Chasing the onset of strange-quark thermalization at the LHC, Report No. ALICE-PUBLIC-2023-003, CERN, 2023, <https://cds.cern.ch/record/2869064>.
- [39] T. Nonaka, M. Kitazawa, and S. I. Esumi, More efficient formulas for efficiency correction of cumulants and effect of using averaged efficiency, *Phys. Rev. C* **95**, 064912 (2017); **103**, 029901(E) (2021).
- [40] T. Pierog, I. Karpenko, J. M. Katzy, E. Yatsenko, and K. Werner, EPOS LHC: Test of collective hadronization with data measured at the CERN Large Hadron Collider, *Phys. Rev. C* **92**, 034906 (2015).
- [41] X.-N. Wang and M. Gyulassy, HIJING: A Monte Carlo model for multiple jet production in pp, pA and AA collisions, *Phys. Rev. D* **44**, 3501 (1991).
- [42] S. Agostinelli *et al.* (GEANT4 Collaboration), GEANT4—a simulation toolkit, *Nucl. Instrum. Methods Phys. Res., Sect. A* **506**, 250 (2003).
- [43] A. Pandav, D. Mallick, and B. Mohanty, Effect of limited statistics on higher order cumulants measurement in heavy-ion collision experiments, *Nucl. Phys. A* **991**, 121608 (2019).
- [44] J. Adam *et al.* (ALICE Collaboration), Centrality dependence of the charged-particle multiplicity density at mid-rapidity in Pb–Pb collisions at $\sqrt{s_{NN}} = 5.02$ TeV, *Phys. Rev. Lett.* **116**, 222302 (2016).
- [45] S. Acharya *et al.* (ALICE Collaboration), Production of light (anti)nuclei in pp collisions at $\sqrt{s} = 5.02$ TeV, *Eur. Phys. J. C* **82**, 289 (2022).
- [46] V. Vovchenko and H. Stoecker, Thermal-FIST: A package for heavy-ion collisions and hadronic equation of state, *Comput. Phys. Commun.* **244**, 295 (2019).
- [47] C. Bierlich, G. Gustafson, L. Lönnblad, and H. Shah, The Angantyr model for heavy-ion collisions in PYTHIA8, *J. High Energy Phys.* **10** (2018) 134.
- [48] V. Vovchenko and V. Koch, Particization of an interacting hadron resonance gas with global conservation laws for event-by-event fluctuations in heavy-ion collisions, *Phys. Rev. C* **103**, 044903 (2021).
- [49] S. Acharya *et al.* (ALICE Collaboration), First measurement of antideuteron number fluctuations at energies available at the large hadron collider, *Phys. Rev. Lett.* **131**, 041901 (2023).
- [50] K.-J. Sun and C. M. Ko, Event-by-event antideuteron multiplicity fluctuation in Pb + Pb collisions at $\sqrt{s_{NN}} = 5.02$ TeV, *Phys. Lett. B* **840**, 137864 (2023).
- [51] S. Gupta, D. Mallick, D. K. Mishra, B. Mohanty, and N. Xu, Limits of thermalization in relativistic heavy ion collisions, *Phys. Lett. B* **829**, 137021 (2022).
- [52] A. Bazavov *et al.*, The QCD equation of state to $\mathcal{O}(\mu_B^6)$ from lattice QCD, *Phys. Rev. D* **95**, 054504 (2017).
- [53] P. Braun-Munzinger, K. Redlich, A. Rustamov, and J. Stachel, The imprint of conservation laws on correlated particle production, *J. High Energy Phys.* **08** (2024) 113.
- [54] S. Acharya *et al.* (ALICE Collaboration), Closing in on critical net-baryon fluctuations at LHC energies: Cumulants up to third order in Pb–Pb collisions, *Phys. Lett. B* **844**, 137545 (2023).

End Matter

Appendix—

Systemic uncertainties: The systematic uncertainties on both $\rho_{\Delta\Xi\Delta K}$ and $\kappa_2(\Delta\Xi)/\kappa_1(\Xi^+ + \Xi^-)$ are summarized in Table I. The contributions associated to the different sources are separately reported. The sources considered for charged kaon candidates are the selection on the number of TPC space points per track, the TPC and TOF PID criteria, the selection on the distance of closest approach (DCA) to the primary vertex (PV) of the reconstructed tracks, and the track χ^2 selection for charged kaons. For the Ξ candidates,

TABLE I. Relative systematic uncertainties on the event-by-event observables due to the different sources considered in this Letter. Only the contributions relevant to the employed particle species are reported.

Source	$\rho_{\Delta\Xi\Delta K}$	$\kappa_2(\Delta\Xi)/\kappa_1(\Xi^+ + \Xi^-)$
TPC space points	0.6%	...
PID selections	0.6%	...
DCA to PV	0.6%	...
Track χ^2	0.3%	...
Ξ mass selection	1%	0.3%
BDT	1%	0.2%

the systematic sources are the applied BDT threshold and the invariant-mass selection.

V_c determination: The best estimate of the correlation volume, V_c , for quantum number conservation in CE SHM is extracted from the data by comparing the experimental results to SHM model predictions based on different values of V_c . This study is performed in the multiplicity region corresponding to Pb–Pb collisions, where the approximation $\gamma_s \approx 1$ holds, by varying the correlation volume in the range $1.0 \leq V_c \leq 4.0$ dV/dy with a step of $\Delta V_c = 0.5$ dV/dy [38]. The step is decreased close to the minimum of the χ^2 profile to obtain a better sampling in that region. The chemical freeze-out temperature is set to $T_{\text{chem}} = 155$ MeV. The quantum numbers that are conserved over V_c are the baryon number, B , and strangeness, S . The latter has a larger effect on the magnitude of the anticorrelation between the net-kaon and net- Ξ numbers. The agreement between the experimental measurements and the model predictions is quantified by a combined χ^2 that simultaneously accounts for the discrepancy between model predictions and data for both the analyzed observables. The six multiplicity intervals corresponding to the results in Pb–Pb collisions are used in this comparison, consisting of 12 data points in total for $\rho_{\Delta\Xi\Delta K}$ and the

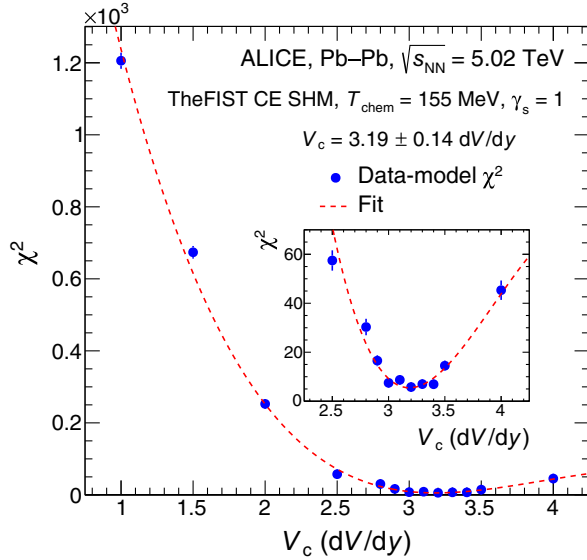


FIG. 2. Combined χ^2 profile for the extraction of the correlation volume for baryon and strangeness conservation obtained by comparing the normalized second order net- Ξ cumulants and the $\rho_{\Delta\Xi\Delta K}$ in Pb-Pb collisions to the Thermal-FIST predictions. The region close to the minimum χ^2 is shown in the inset. The dashed line represents a fit to the χ^2 profile with a fourth-degree polynomial function.

κ_2/κ_1 ratio. The χ^2 calculation takes into account only the statistical uncertainties. The obtained χ^2 profile as a function of V_c is shown in Fig. 2. The observed χ^2 is dominated by $\rho_{\Delta\Xi\Delta K}$ because it has smaller uncertainties with respect to the κ_2/κ_1 ratio of the net- Ξ number. The systematic uncertainties on $\rho_{\Delta\Xi\Delta K}$ and $\kappa_2/\kappa_1(\Delta\Xi)$ are also included in the V_c evaluation assuming full correlation of the systematic uncertainties with multiplicity. The assigned uncertainty is obtained as half of the difference between the V_c values obtained by repeating the fit, shifting upward and downward the event-by-event observables by their systematic uncertainties. The final uncertainty on V_c is obtained by adding the statistical

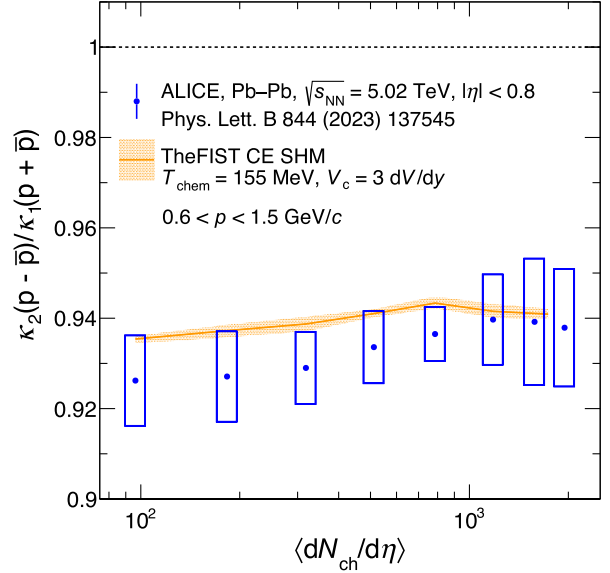


FIG. 3. Comparison between the net-proton normalized second-order cumulant as a function of the average multiplicity at midrapidity measured by the ALICE Collaboration in Pb-Pb collisions at $\sqrt{s_{NN}} = 5.02$ TeV (blue circles) [54] and the predictions of the Thermal-FIST model, with $T_{\text{chem}} = 155$ MeV and $V_c = 3$ dV/dy (orange band).

and systematic contributions in quadrature. The correlation volume obtained from the minimization of the observed χ^2 profile is $V_c = 3.19 \pm 0.14$ dV/dy, with a fit probability of $P = 0.94$.

Comparison to net-proton fluctuations: In Fig. 3, the comparison between the published κ_2/κ_1 normalized second-order cumulant of net protons and the model calculations obtained with the Thermal-FIST model is shown. In the model parametrization, the chemical freeze-out temperature and the strangeness saturation factor are set to $T_{\text{chem}} = 155$ MeV and $\gamma_s = 1$, respectively. The parametrization of the system volume per unit of rapidity, dV/dy, is obtained from Ref. [15].

S. Acharya¹²⁷, D. Adamová⁸⁶, A. Agarwal¹³⁵, G. Aglieri Rinella³², L. Aglietta²⁴, M. Agnello²⁹, N. Agrawal²⁵, Z. Ahammed¹³⁵, S. Ahmad¹⁵, S. U. Ahn⁷¹, I. Ahuja³⁷, A. Akindinov¹⁴¹, V. Akishina³⁸, M. Al-Turany⁹⁷, D. Aleksandrov¹⁴¹, B. Alessandro⁵⁶, H. M. Alfanda⁶, R. Alfaro Molina⁶⁷, B. Ali¹⁵, A. Alici²⁵, N. Alizadehvandchali¹¹⁶, A. Alkin¹⁰⁴, J. Alme²⁰, G. Alocco⁵², T. Alt⁶⁴, A. R. Altamura⁵⁰, I. Altsybeev⁹⁵, J. R. Alvarado⁴⁴, C. O. R. Alvarez⁴⁴, M. N. Anaam⁶, C. Andrei⁴⁵, N. Andreou¹¹⁵, A. Andronic¹²⁶, E. Andronov¹⁴¹, V. Anguelov⁹⁴, F. Antinori⁵⁴, P. Antonioli⁵¹, N. Apadula⁷⁴, L. Aphecetche¹⁰³, H. Appelshäuser⁶⁴, C. Arata⁷³, S. Arcelli²⁵, M. Aresti²², R. Arnaldi⁵⁶, J. G. M. C. A. Arneiro¹¹⁰, I. C. Arsene¹⁹, M. Arslandok¹³⁸, A. Augustinus³², R. Averbeck⁹⁷, D. Averyanov¹⁴¹, M. D. Azmi¹⁵, H. Baba¹²⁴, A. Badalà⁵³

J. Bae¹⁰⁴, Y. W. Baek⁴⁰, X. Bai¹²⁰, R. Bailhache⁶⁴, Y. Bailung⁴⁸, R. Bala⁹¹, A. Balbino²⁹, A. Baldisseri¹³⁰,
 B. Balis², D. Banerjee⁴, Z. Banoo⁹¹, V. Barbasova³⁷, F. Barile³¹, L. Barioglio⁵⁶, M. Barlou⁷⁸, B. Barman⁴¹,
 G. G. Barnaföldi⁴⁶, L. S. Barnby¹¹⁵, E. Barreau¹⁰³, V. Barret¹²⁷, L. Barreto¹¹⁰, C. Bartels¹¹⁹, K. Barth³²,
 E. Bartsch⁶⁴, N. Bastid¹²⁷, S. Basu⁷⁵, G. Batigne¹⁰³, D. Battistini⁹⁵, B. Batyunya¹⁴², D. Bauri⁴⁷,
 J. L. Bazo Alba¹⁰¹, I. G. Bearden⁸³, C. Beattie¹³⁸, P. Becht⁹⁷, D. Behera⁴⁸, I. Belikov¹²⁹,
 A. D. C. Bell Hechavarria¹²⁶, F. Bellini²⁵, R. Bellwied¹¹⁶, S. Belokurova¹⁴¹, L. G. E. Beltran¹⁰⁹,
 Y. A. V. Beltran⁴⁴, G. Bencedi⁴⁶, A. Bensaoula¹¹⁶, S. Beole²⁴, Y. Berdnikov¹⁴¹, A. Berdnikova⁹⁴, L. Bergmann⁹⁴,
 M. G. Besoiu⁶³, L. Betev³², P. P. Bhaduri¹³⁵, A. Bhasin⁹¹, B. Bhattacharjee⁴¹, L. Bianchi²⁴, N. Bianchi⁴⁹,
 J. Bielčík³⁵, J. Bielčíková⁸⁶, A. P. Bigot¹²⁹, A. Bilandzic⁹⁵, G. Biro⁴⁶, S. Biswas⁴, N. Bize¹⁰³, J. T. Blair¹⁰⁸,
 D. Blau¹⁴¹, M. B. Blidaru⁹⁷, N. Bluhme³⁸, C. Blume⁶⁴, G. Boca^{21,55}, F. Bock⁸⁷, T. Bodova²⁰, J. Bok¹⁶,
 L. Boldizsár⁴⁶, M. Bombara³⁷, P. M. Bond³², G. Bonomi^{55,134}, H. Borel¹³⁰, A. Borissov¹⁴¹,
 A. G. Borquez Carcamo⁹⁴, H. Bossi¹³⁸, E. Botta²⁴, Y. E. M. Bouziani⁶⁴, L. Bratrud⁶⁴, P. Braun-Munzinger⁹⁷,
 M. Bregant¹¹⁰, M. Broz³⁵, G. E. Bruno^{31,96}, V. D. Buchakchiev³⁶, M. D. Buckland²³, D. Budnikov¹⁴¹,
 H. Buesching⁶⁴, S. Bufalino²⁹, P. Buhler¹⁰², N. Burmasov¹⁴¹, Z. Buthelezi^{68,123}, A. Bylinkin²⁰, S. A. Bysiak¹⁰⁷,
 J. C. Cabanillas Noris¹⁰⁹, M. F. T. Cabrera¹¹⁶, M. Cai⁶, H. Caines¹³⁸, A. Caliva²⁸, E. Calvo Villar¹⁰¹,
 J. M. M. Camacho¹⁰⁹, P. Camerini²³, F. D. M. Canedo¹¹⁰, S. L. Cantway¹³⁸, M. Carabas¹¹³, A. A. Carballo³²,
 F. Carnesecchi³², R. Caron¹²⁸, L. A. D. Carvalho¹¹⁰, J. Castillo Castellanos¹³⁰, M. Castoldi³², F. Catalano³²,
 S. Cattaruzzi²³, C. Ceballos Sanchez¹⁴², R. Cerri²⁴, I. Chakaberia⁷⁴, P. Chakraborty^{47,136}, S. Chandra¹³⁵,
 S. Chapeland³², M. Chartier¹¹⁹, S. Chattopadhyay¹³⁵, S. Chattopadhyay¹³⁵, S. Chattopadhyay⁹⁹, M. Chen³⁹,
 T. Cheng^{6,97}, C. Cheshkov¹²⁸, V. Chibante Barroso³², D. D. Chinellato¹¹¹, E. S. Chizzali^{95,b}, J. Cho⁵⁸, S. Cho⁵⁸,
 P. Chochula³², Z. A. Chochulska¹³⁶, D. Choudhury⁴¹, P. Christakoglou⁸⁴, C. H. Christensen⁸³, P. Christiansen⁷⁵,
 T. Chujo¹²⁵, M. Ciacco²⁹, C. Cicalo⁵², M. R. Ciupek⁹⁷, G. Clai^{51,c}, F. Colamaria⁵⁰, J. S. Colburn¹⁰⁰, D. Colella³¹,
 M. Colocci²⁵, M. Concas³², G. Conesa Balbastre⁷³, Z. Conesa del Valle¹³¹, G. Contin²³, J. G. Contreras³⁵,
 M. L. Coquet^{103,130}, P. Cortese^{56,133}, M. R. Cosentino¹¹², F. Costa³², S. Costanza^{21,55}, C. Cot¹³¹, J. Crkovská⁹⁴,
 P. Crochet¹²⁷, R. Cruz-Torres⁷⁴, P. Cui⁶, M. M. Czarnynoga¹³⁶, A. Dainese⁵⁴, G. Dange³⁸, M. C. Danisch⁹⁴,
 A. Danu⁶³, P. Das⁸⁰, P. Das⁴, S. Das⁴, A. R. Dash¹²⁶, S. Dash⁴⁷, A. De Caro²⁸, G. de Cataldo⁵⁰,
 J. de Cuveland³⁸, A. De Falco²², D. De Gruttola²⁸, N. De Marco⁵⁶, C. De Martin²³, S. De Pasquale²⁸, R. Deb¹³⁴,
 R. Del Grande⁹⁵, L. Dello Stritto³², W. Deng⁶, K. C. Devereaux¹⁸, P. Dhankher¹⁸, D. Di Bari³¹, A. Di Mauro³²,
 B. Diab¹³⁰, R. A. Diaz^{7,142}, T. Dietel¹¹⁴, Y. Ding⁶, J. Ditzel⁶⁴, R. Divià³², Ø. Djuvsland²⁰, U. Dmitrieva¹⁴¹,
 A. Dobrin⁶³, B. Dönigus⁶⁴, J. M. Dubinski¹³⁶, A. Dubla⁹⁷, P. Dupieux¹²⁷, N. Dzalaiova¹³, T. M. Eder¹²⁶,
 R. J. Ehlers⁷⁴, F. Eisenhut⁶⁴, R. Ejima⁹², D. Elia⁵⁰, B. Erazmus¹⁰³, F. Ercolessi²⁵, B. Espagnon¹³¹, G. Eulisse³²,
 D. Evans¹⁰⁰, S. Evdokimov¹⁴¹, L. Fabbietti⁹⁵, M. Faggin²³, J. Faivre⁷³, F. Fan⁶, W. Fan⁷⁴, A. Fantoni⁴⁹,
 M. Fasel⁸⁷, A. Feliciello⁵⁶, G. Feofilov¹⁴¹, A. Fernández Téllez⁴⁴, L. Ferrandi¹¹⁰, M. B. Ferrer³², A. Ferrero¹³⁰,
 C. Ferrero^{56,d}, A. Ferretti²⁴, V. J. G. Feuillard⁹⁴, V. Filova³⁵, D. Finogeev¹⁴¹, F. M. Fionda⁵², E. Flatland³²,
 F. Flor^{116,138}, A. N. Flores¹⁰⁸, S. Foertsch⁶⁸, I. Fokin⁹⁴, S. Fokin¹⁴¹, U. Follo^{56,d}, E. Fragiaco⁵⁷, E. Frajna⁴⁶,
 U. Fuchs³², N. Funicello²⁸, C. Furget⁷³, A. Furs¹⁴¹, T. Fusayasu⁹⁸, J. J. Gaardhøje⁸³, M. Gagliardi²⁴,
 A. M. Gago¹⁰¹, T. Gahlaut⁴⁷, C. D. Galvan¹⁰⁹, D. R. Gangadharan¹¹⁶, P. Ganoti⁷⁸, C. Garabatos⁹⁷, J. M. Garcia⁴⁴,
 T. García Chávez⁴⁴, E. Garcia-Solis⁹, C. Gargiulo³², P. Gasik⁹⁷, H. M. Gaur³⁸, A. Gautam¹¹⁸, M. B. Gay Ducati⁶⁶,
 M. Germain¹⁰³, R. A. Gernhauser⁹⁵, C. Ghosh¹³⁵, M. Giacalone⁵¹, G. Gioachin²⁹, S. K. Giri¹³⁵, P. Giubellino^{56,97},
 P. Giubileo²⁷, A. M. C. Glaenger¹³⁰, P. Glässel⁹⁴, E. Glimos¹²², D. J. Q. Goh⁷⁶, V. Gonzalez¹³⁷, P. Gordeev¹⁴¹,
 M. Gorgon², K. Goswami⁴⁸, S. Gotovac³³, V. Grabski⁶⁷, L. K. Graczykowski¹³⁶, E. Grecka⁸⁶, A. Grelli⁵⁹,
 C. Grigoras³², V. Grigoriev¹⁴¹, S. Grigoryan^{1,142}, F. Grosa³², J. F. Grosse-Oetringhaus³², R. Grosso⁹⁷,
 D. Grund³⁵, N. A. Grunwald⁹⁴, G. G. Guardiano¹¹¹, R. Guernane⁷³, M. Guilbaud¹⁰³, K. Gulbrandsen⁸³,
 J. J. W. K. Gumprecht¹⁰², T. Gündem⁶⁴, T. Gunji¹²⁴, W. Guo⁶, A. Gupta⁹¹, R. Gupta⁹¹, R. Gupta⁴⁸,
 K. Gwizdziel¹³⁶, L. Gyulai⁴⁶, C. Hadjidakis¹³¹, F. U. Haider⁹¹, S. Haidlova³⁵, M. Haldar⁴, H. Hamagaki⁷⁶,
 A. Hamdi⁷⁴, Y. Han¹³⁹, B. G. Hanley¹³⁷, R. Hannigan¹⁰⁸, J. Hansen⁷⁵, M. R. Haque⁹⁷, J. W. Harris¹³⁸,
 A. Harton⁹, M. V. Hartung⁶⁴, H. Hassan¹¹⁷, D. Hatzifotiadou⁵¹, P. Hauer⁴², L. B. Havener¹³⁸, E. Hellbär⁹⁷,
 H. Helstrup³⁴, M. Hemmer⁶⁴, T. Herman³⁵, S. G. Hernandez¹¹⁶, G. Herrera Corral⁸, S. Herrmann¹²⁸,
 K. F. Hetland³⁴, B. Heybeck⁶⁴, H. Hillemanns³², B. Hippolyte¹²⁹, F. W. Hoffmann⁷⁰, B. Hofman⁵⁹

G. H. Hong¹³⁹ M. Horst⁹⁵ A. Horzyk² Y. Hou⁶ P. Hristov³² P. Huhn⁶⁴ L. M. Huhta¹¹⁷ T. J. Humanic⁸⁸
A. Hutson¹¹⁶ D. Hutter³⁸ M. C. Hwang¹⁸ R. Ilkaev¹⁴¹ M. Inaba¹²⁵ G. M. Innocenti³² M. Ippolitov¹⁴¹
A. Isakov⁸⁴ T. Isidori¹¹⁸ M. S. Islam⁹⁹ S. Iurchenko¹⁴¹ M. Ivanov¹³ M. Ivanov⁹⁷ V. Ivanov¹⁴¹ K. E. Iversen⁷⁵
M. Jablonski² B. Jacak^{18,74} N. Jacazio²⁵ P. M. Jacobs⁷⁴ S. Jadlovska¹⁰⁶ J. Jadlovsky¹⁰⁶ S. Jaelani⁸²
C. Jahnke¹¹⁰ M. J. Jakubowska¹³⁶ M. A. Janik¹³⁶ T. Janson⁷⁰ S. Ji¹⁶ S. Jia¹⁰ A. A. P. Jimenez⁶⁵ F. Jonas⁷⁴
D. M. Jones¹¹⁹ J. M. Jowett^{32,97} J. Jung⁶⁴ M. Jung⁶⁴ A. Junique³² A. Jusko¹⁰⁰ J. Kaewjai¹⁰⁵ P. Kalinak⁶⁰
A. Kalweit³² A. Karasu Uysal^{72,e} D. Karatovic⁸⁹ N. Karatzenis¹⁰⁰ O. Karavichev¹⁴¹ T. Karavicheva¹⁴¹
E. Karpechev¹⁴¹ M. J. Karwowska^{32,136} U. Kebschull⁷⁰ R. Keidel¹⁴⁰ M. Keil³² B. Ketzer⁴² S. S. Khade⁴⁸
A. M. Khan¹²⁰ S. Khan¹⁵ A. Khanzadeev¹⁴¹ Y. Kharlov¹⁴¹ A. Khatun¹¹⁸ A. Khuntia³⁵ Z. Khuranova⁶⁴
B. Kileng³⁴ B. Kim¹⁰⁴ C. Kim¹⁶ D. J. Kim¹¹⁷ E. J. Kim⁶⁹ J. Kim¹³⁹ J. Kim⁵⁸ J. Kim^{32,69} M. Kim¹⁸
S. Kim¹⁷ T. Kim¹³⁹ K. Kimura⁹² A. Kirkova³⁶ S. Kirsch⁶⁴ I. Kisel³⁸ S. Kiselev¹⁴¹ A. Kisiel¹³⁶
J. P. Kitowski² J. L. Klay⁵ J. Klein³² S. Klein⁷⁴ C. Klein-Bösing¹²⁶ M. Kleiner⁶⁴ T. Klemenz⁹⁵
A. Kluge³² C. Kobdaj¹⁰⁵ R. Kohara¹²⁴ T. Kollegger⁹⁷ A. Kondratyev¹⁴² N. Kondratyeva¹⁴¹ J. König⁶⁴
S. A. Königstorfer⁹⁵ P. J. Konopka³² G. Kornakov¹³⁶ M. Korwieser⁹⁵ S. D. Koryciak² C. Koster⁸⁴
A. Kotliarov⁸⁶ N. Kovacic⁸⁹ V. Kovalenko¹⁴¹ M. Kowalski¹⁰⁷ V. Kozuharov³⁶ I. Králik⁶⁰ A. Kravčáková³⁷
L. Krcal^{32,38} M. Krivda^{60,100} F. Krizek⁸⁶ K. Krizkova Gajdosova³² C. Krug⁶⁶ M. Krüger⁶⁴ D. M. Krupova³⁵
E. Kryshen¹⁴¹ V. Kučera⁵⁸ C. Kuhn¹²⁹ P. G. Kuijer⁸⁴ T. Kumaoka¹²⁵ D. Kumar¹³⁵ L. Kumar⁹⁰ N. Kumar⁹⁰
S. Kumar³¹ S. Kundu³² P. Kurashvili⁷⁹ A. Kurepin¹⁴¹ A. B. Kurepin¹⁴¹ A. Kuryakin¹⁴¹ S. Kushpil⁸⁶
V. Kuskov¹⁴¹ M. Kutyla¹³⁶ A. Kuznetsov¹⁴² M. J. Kweon⁵⁸ Y. Kwon¹³⁹ S. L. La Pointe³⁸ P. La Rocca²⁶
A. Lakrathok¹⁰⁵ M. Lamanna³² A. R. Landou⁷³ R. Langoy¹²¹ P. Larionov³² E. Laudi³² L. Lautner^{32,95}
R. A. N. Laveaga¹⁰⁹ R. Lavicka¹⁰² R. Lea^{55,134} H. Lee¹⁰⁴ I. Legrand⁴⁵ G. Legras¹²⁶ J. Lehrbach³⁸
A. M. Lejeune³⁵ T. M. Lelek² R. C. Lemmon^{85,a} I. León Monzón¹⁰⁹ M. M. Lesch⁹⁵ E. D. Lesser¹⁸ P. Lévai⁴⁶
M. Li⁶ X. Li¹⁰ B. E. Liang-gilman¹⁸ J. Lien¹²¹ R. Lietava¹⁰⁰ I. Likmeta¹¹⁶ B. Lim²⁴ S. H. Lim¹⁶
V. Lindenstruth³⁸ A. Lindner⁴⁵ C. Lippmann⁹⁷ D. H. Liu⁶ J. Liu¹¹⁹ G. S. S. Liveraro¹¹¹ I. M. Lofnes²⁰
C. Loizides⁸⁷ S. Lokos¹⁰⁷ J. Lömker⁵⁹ X. Lopez¹²⁷ E. López Torres⁷ C. Lotteau¹²⁸ P. Lu^{97,120} F. V. Lugo⁶⁷
J. R. Luhder¹²⁶ M. Lunardon²⁷ G. Luparello⁵⁷ Y. G. Ma³⁹ M. Mager³² A. Maire¹²⁹ E. M. Majerz²
M. V. Makariev³⁶ M. Malaev¹⁴¹ G. Malfattore²⁵ N. M. Malik⁹¹ Q. W. Malik¹⁹ S. K. Malik⁹¹ L. Malinina^{142,a,f}
D. Mallick¹³¹ N. Mallick⁴⁸ G. Mandaglio^{30,53} S. K. Mandal⁷⁹ A. Manea⁶³ V. Manko¹⁴¹ F. Manso¹²⁷
V. Manzari⁵⁰ Y. Mao⁶ R. W. Marcjan² G. V. Margagliotti²³ A. Margotti⁵¹ A. Marín⁹⁷ C. Markert¹⁰⁸
P. Martinengo³² M. I. Martínez⁴⁴ G. Martínez García¹⁰³ M. P. P. Martins¹¹⁰ S. Masciocchi⁹⁷ M. Maserà²⁴
A. Masoni⁵² L. Massacrier¹³¹ O. Massen⁵⁹ A. Mastroserio^{50,132} O. Matonoha⁷⁵ S. Mattiazzo²⁷ A. Matyja¹⁰⁷
A. L. Mazuecos³² F. Mazzaschi^{24,32} M. Mazzilli¹¹⁶ J. E. Mdhluli¹²³ Y. Melikyan⁴³ M. Melo¹¹⁰
A. Menchaca-Rocha⁶⁷ J. E. M. Mendez⁶⁵ E. Meninno¹⁰² A. S. Menon¹¹⁶ M. W. Menzel^{32,94} M. Meres¹³
Y. Miake¹²⁵ L. Micheletti³² D. L. Mihaylov⁹⁵ K. Mikhaylov^{141,142} N. Minafra¹¹⁸ D. Miśkowiec⁹⁷
A. Modak^{4,134} B. Mohanty⁸⁰ M. Mohisin Khan^{15,g} M. A. Molander⁴³ S. Monira¹³⁶ C. Mordasini¹¹⁷
D. A. Moreira De Godoy¹²⁶ I. Morozov¹⁴¹ A. Morsch³² T. Mrnjavac³² V. Muccifora⁴⁹ S. Muhuri¹³⁵
J. D. Mulligan⁷⁴ A. Mulliri²² M. G. Munhoz¹¹⁰ R. H. Munzer⁶⁴ H. Murakami¹²⁴ S. Murray¹¹⁴ L. Musa³²
J. Musinsky⁶⁰ J. W. Myrcha¹³⁶ B. Naik¹²³ A. I. Nambrath¹⁸ B. K. Nandi⁴⁷ R. Nania⁵¹ E. Nappi⁵⁰
A. F. Nassirpour¹⁷ A. Nath⁹⁴ S. Nath¹³⁵ C. Nattrass¹²² M. N. Naydenov³⁶ A. Neagu¹⁹ A. Negru¹¹³
E. Nekrasova¹⁴¹ L. Nellen⁶⁵ R. Nepeivoda⁷⁵ S. Nese¹⁹ G. Neskovic³⁸ N. Nicassio⁵⁰ B. S. Nielsen⁸³
E. G. Nielsen⁸³ S. Nikolaev¹⁴¹ S. Nikulin¹⁴¹ V. Nikulin¹⁴¹ F. Noferini⁵¹ S. Noh¹² P. Nomokonov¹⁴²
J. Norman¹¹⁹ N. Novitzky⁸⁷ P. Nowakowski¹³⁶ A. Nyanin¹⁴¹ J. Nystrand²⁰ S. Oh¹⁷ A. Ohlson⁷⁵
V. A. Okorokov¹⁴¹ J. Oleniacz¹³⁶ A. Onnerstad¹¹⁷ C. Oppedisano⁵⁶ A. Ortiz Velasquez⁶⁵ J. Otwinowski¹⁰⁷
M. Oya⁹² K. Oyama⁷⁶ Y. Pachmayer⁹⁴ S. Padhan⁴⁷ D. Pagano^{55,134} G. Paić⁶⁵ S. Paisano-Guzmán⁴⁴
A. Palasciano⁵⁰ S. Panebianco¹³⁰ C. Pantouvakis²⁷ H. Park¹²⁵ H. Park¹⁰⁴ J. Park¹²⁵ J. E. Parkkila³²
Y. Patley⁴⁷ R. N. Patra⁵⁰ B. Paul¹³⁵ H. Pei⁶ T. Peitzmann⁵⁹ X. Peng¹¹ M. Pennisi²⁴ S. Perciballi²⁴
D. Peresunko¹⁴¹ G. M. Perez⁷ Y. Pestov¹⁴¹ M. T. Petersen⁸³ V. Petrov¹⁴¹ M. Petrovici⁴⁵ S. Piano⁵⁷ M. Pikna¹³
P. Pillot¹⁰³ O. Pinazza^{32,51} L. Pinsky¹¹⁶ C. Pinto⁹⁵ S. Pisano⁴⁹ M. Płoskoń⁷⁴ M. Planinic⁸⁹ F. Pliquett⁶⁴
D. K. Plociennik² M. G. Poghosyan⁸⁷ B. Polichtchouk¹⁴¹ S. Politano²⁹ N. Poljak⁸⁹ A. Pop⁴⁵

S. Porteboeuf-Houssais¹²⁷ V. Pozdniakov^{142,a} I. Y. Pozos⁴⁴ K. K. Pradhan⁴⁸ S. K. Prasad⁴ S. Prasad⁴⁸
R. Preghenella⁵¹ F. Prino⁵⁶ C. A. Pruneau¹³⁷ I. Pshenichnov¹⁴¹ M. Puccio³² S. Pucillo²⁴ S. Qiu⁸⁴
L. Quaglia²⁴ S. Ragoni¹⁴ A. Rai¹³⁸ A. Rakotozafindrabe¹³⁰ L. Ramello^{56,133} F. Rami¹²⁹ M. Rasa²⁶
S. S. Räsänen⁴³ R. Rath⁵¹ M. P. Rauch²⁰ I. Ravasenga³² K. F. Read^{87,122} C. Reckziegel¹¹²
A. R. Redelbach³⁸ K. Redlich^{79,h} C. A. Reetz⁹⁷ H. D. Regules-Medel⁴⁴ A. Rehman²⁰ F. Reidt³²
H. A. Reme-Ness³⁴ Z. Rescakova³⁷ K. Reygers⁹⁴ A. Riabov¹⁴¹ V. Riabov¹⁴¹ R. Ricci²⁸ M. Richter²⁰
A. A. Riedel⁹⁵ W. Riegler³² A. G. Riffero²⁴ M. Rignanese²⁷ C. Ripoli²⁸ C. Ristea⁶³ M. V. Rodriguez³²
M. Rodríguez Cahuantzi⁴⁴ S. A. Rodríguez Ramírez⁴⁴ K. Røed¹⁹ R. Rogalev¹⁴¹ E. Rogochaya¹⁴²
T. S. Rogoschinski⁶⁴ D. Rohr³² D. Röhrich²⁰ S. Rojas Torres³⁵ P. S. Rokita¹³⁶ G. Romanenko²⁵
F. Ronchetti⁴⁹ E. D. Rosas⁶⁵ K. Roslon¹³⁶ A. Rossi⁵⁴ A. Roy⁴⁸ S. Roy⁴⁷ N. Rubini^{25,51} J. A. Rudolph⁸⁴
D. Ruggiano¹³⁶ R. Rui²³ P. G. Russek² R. Russo⁸⁴ A. Rustamov⁸¹ E. Ryabinkin¹⁴¹ Y. Ryabov¹⁴¹
A. Rybicki¹⁰⁷ J. Ryu¹⁶ W. Rzeska¹³⁶ B. Sabiu⁵¹ S. Sadovsky¹⁴¹ J. Saetre²⁰ K. Šafařík³⁵ S. K. Saha⁴
S. Saha⁸⁰ B. Sahoo⁴⁸ R. Sahoo⁴⁸ S. Sahoo⁶¹ D. Sahu⁴⁸ P. K. Sahu⁶¹ J. Saini¹³⁵ K. Sajdakova³⁷ S. Sakai¹²⁵
M. P. Salvan⁹⁷ S. Sambyal⁹¹ D. Samitz¹⁰² I. Sanna^{32,95} T. B. Saramela¹¹⁰ D. Sarkar⁸³ P. Sarma⁴¹
V. Sarritsu²² V. M. Sarti⁹⁵ M. H. P. Sas³² S. Sawan⁸⁰ E. Scapparone⁵¹ J. Schambach⁸⁷ H. S. Scheid⁶⁴
C. Schiaua⁴⁵ R. Schicker⁹⁴ F. Schlepper⁹⁴ A. Schmah⁹⁷ C. Schmidt⁹⁷ H. R. Schmidt⁹³ M. O. Schmidt³²
M. Schmidt⁹³ N. V. Schmidt⁸⁷ A. R. Schmier¹²² R. Schotter¹²⁹ A. Schröter³⁸ J. Schukraft³² K. Schweda⁹⁷
G. Scioli²⁵ E. Scomparin⁵⁶ J. E. Seger¹⁴ Y. Sekiguchi¹²⁴ D. Sekihata¹²⁴ M. Selina⁸⁴ I. Selyuzhenkov⁹⁷
S. Senyukov¹²⁹ J. J. Seo⁹⁴ D. Serebryakov¹⁴¹ L. Serkin⁶⁵ L. Šerkšnytė⁹⁵ A. Sevcenco⁶³ T. J. Shaba⁶⁸
A. Shabetai¹⁰³ R. Shahoyan³² A. Shangaraev¹⁴¹ B. Sharma⁹¹ D. Sharma⁴⁷ H. Sharma⁵⁴ M. Sharma⁹¹
S. Sharma⁷⁶ S. Sharma⁹¹ U. Sharma⁹¹ A. Shatat¹³¹ O. Sheibani¹¹⁶ K. Shigaki⁹² M. Shimomura⁷⁷ J. Shin¹²
S. Shirinkin¹⁴¹ Q. Shou³⁹ Y. Sibiriak¹⁴¹ S. Siddhanta⁵² T. Siemiarz⁷⁹ T. F. Silva¹¹⁰ D. Silvermyr⁷⁵
T. Simantathammakul¹⁰⁵ R. Simeonov³⁶ B. Singh⁹¹ B. Singh⁹⁵ K. Singh⁴⁸ R. Singh⁸⁰ R. Singh⁹¹ R. Singh⁹⁷
S. Singh¹⁵ V. K. Singh¹³⁵ V. Singhal¹³⁵ T. Sinha⁹⁹ B. Sitar¹³ M. Sitta^{56,133} T. B. Skaali¹⁹ G. Skorodumovs⁹⁴
N. Smirnov¹³⁸ R. J. M. Snellings⁵⁹ E. H. Solheim¹⁹ J. Song¹⁶ C. Sonnabend^{32,97} J. M. Sonneveld⁸⁴
F. Soramel²⁷ A. B. Soto-hernandez⁸⁸ R. Spijkers⁸⁴ I. Sputowska¹⁰⁷ J. Staa⁷⁵ J. Stachel⁹⁴ I. Stan⁶³
P. J. Steffanic¹²² S. F. Stiefelmaier⁹⁴ D. Stocco¹⁰³ I. Storehaug¹⁹ N. J. Strangmann⁶⁴ P. Stratmann¹²⁶
S. Strazzi²⁵ A. Sturmiolo^{30,53} C. P. Stylianidis⁸⁴ A. A. P. Suaide¹¹⁰ C. Suire¹³¹ M. Sukhanov¹⁴¹ M. Suljic³²
R. Sultanov¹⁴¹ V. Sumberia⁹¹ S. Sumowidagdo⁸² I. Szarka¹³ M. Szymkowski¹³⁶ S. F. Taghavi⁹⁵
G. Taillepiéd⁹⁷ J. Takahashi¹¹¹ G. J. Tambave⁸⁰ S. Tang⁶ Z. Tang¹²⁰ J. D. Tapia Takaki¹¹⁸ N. Tapus¹¹³
L. A. Tarasovicova¹²⁶ M. G. Tazila⁴⁵ G. F. Tassielli³¹ A. Tauro³² A. Tavira García¹³¹ G. Tejada Muñoz⁴⁴
A. Telesca³² L. Terlizzi²⁴ C. Terrevoli⁵⁰ S. Thakur⁴ D. Thomas¹⁰⁸ A. Tikhonov¹⁴¹ N. Tiltmann^{32,126}
A. R. Timmins¹¹⁶ M. Tkacik¹⁰⁶ T. Tkacik¹⁰⁶ A. Toia⁶⁴ R. Tokumoto⁹² S. Tomassini²⁵ K. Tomohiro⁹²
N. Topilskaya¹⁴¹ M. Toppi⁴⁹ V. V. Torres¹⁰³ A. G. Torres Ramos³¹ A. Trifiró^{30,53} T. Triloki⁹⁶
A. S. Triolo^{30,32,53} S. Tripathy³² T. Tripathy⁴⁷ V. Trubnikov³ W. H. Trzaska¹¹⁷ T. P. Trzcinski¹³⁶ C. Tsolanta¹⁹
R. Tu³⁹ A. Tumkin¹⁴¹ R. Turrisi⁵⁴ T. S. Tveter¹⁹ K. Ullaland²⁰ B. Ulukutlu⁹⁵ A. Uras¹²⁸ M. Urioni¹³⁴
G. L. Usai²² M. Vala³⁷ N. Valle⁵⁵ L. V. R. van Doremalen⁵⁹ M. van Leeuwen⁸⁴ C. A. van Veen⁹⁴
R. J. G. van Weelden⁸⁴ P. Vande Vyvre³² D. Varga⁴⁶ Z. Varga⁴⁶ P. Vargas Torres⁶⁵ M. Vasileiou⁷⁸
A. Vasiliev¹⁴¹ O. Vázquez Doce⁴⁹ O. Vazquez Rueda¹¹⁶ V. Vechernin¹⁴¹ E. Vercellin²⁴ S. Vergara Limón⁴⁴
R. Verma⁴⁷ L. Vermunt⁹⁷ R. Vértesi⁴⁶ M. Verweij⁵⁹ L. Vickovic³³ Z. Vilakazi¹²³ O. Villalobos Baillie¹⁰⁰
A. Villani²³ A. Vinogradov¹⁴¹ T. Virgili²⁸ M. M. O. Virta¹¹⁷ A. Vodopyanov¹⁴² B. Volkel³² M. A. Völkl⁹⁴
S. A. Voloshin¹³⁷ G. Volpe³¹ B. von Haller³² I. Vorobyev³² N. Vozniuk¹⁴¹ J. Vrláková³⁷ J. Wan³⁹
C. Wang³⁹ D. Wang³⁹ Y. Wang³⁹ Y. Wang⁶ A. Wegrzynek³² F. T. Weiglhofer³⁸ S. C. Wenzel³²
J. P. Wessels¹²⁶ J. Wiechula⁶⁴ J. Wikne¹⁹ G. Wilk⁷⁹ J. Wilkinson⁹⁷ G. A. Willems¹²⁶ B. Windelband⁹⁴
M. Winn¹³⁰ J. R. Wright¹⁰⁸ W. Wu³⁹ Y. Wu¹²⁰ Z. Xiong¹²⁰ R. Xu⁶ A. Yadav⁴² A. K. Yadav¹³⁵
Y. Yamaguchi⁹² S. Yang²⁰ S. Yano⁹² E. R. Yeats¹⁸ Z. Yin⁶ I.-K. Yoo¹⁶ J. H. Yoon⁵⁸ H. Yu¹² S. Yuan²⁰
A. Yuncu⁹⁴ V. Zaccolo²³ C. Zampolli³² M. Zang⁶ F. Zanone⁹⁴ N. Zardoshti³² A. Zarochentsev¹⁴¹
P. Závada⁶² N. Zaviyalov¹⁴¹ M. Zhalov¹⁴¹ B. Zhang⁶ C. Zhang¹³⁰ L. Zhang³⁹ M. Zhang^{6,127} S. Zhang³⁹

X. Zhang⁶, Y. Zhang,¹²⁰ Z. Zhang⁶, M. Zhao¹⁰, V. Zhrebchevskii¹⁴¹, Y. Zhi,¹⁰ D. Zhou⁶, Y. Zhou⁸³, J. Zhu^{6,54},
S. Zhu,¹²⁰ Y. Zhu,⁶ S. C. Zugravel⁵⁶, and N. Zurlo^{55,134}

(ALICE Collaboration)

- ¹A.I. Alikhanyan National Science Laboratory (Yerevan Physics Institute) Foundation, Yerevan, Armenia
²AGH University of Krakow, Cracow, Poland
³Bogolyubov Institute for Theoretical Physics, National Academy of Sciences of Ukraine, Kiev, Ukraine
⁴Bose Institute, Department of Physics and Centre for Astroparticle Physics and Space Science (CAPSS), Kolkata, India
⁵California Polytechnic State University, San Luis Obispo, California, USA
⁶Central China Normal University, Wuhan, China
⁷Centro de Aplicaciones Tecnológicas y Desarrollo Nuclear (CEADEN), Havana, Cuba
⁸Centro de Investigación y de Estudios Avanzados (CINVESTAV), Mexico City and Mérida, Mexico
⁹Chicago State University, Chicago, Illinois, USA
¹⁰China Institute of Atomic Energy, Beijing, China
¹¹China University of Geosciences, Wuhan, China
¹²Chungbuk National University, Cheongju, Republic of Korea
¹³Comenius University Bratislava, Faculty of Mathematics, Physics and Informatics, Bratislava, Slovak Republic
¹⁴Creighton University, Omaha, Nebraska, USA
¹⁵Department of Physics, Aligarh Muslim University, Aligarh, India
¹⁶Department of Physics, Pusan National University, Pusan, Republic of Korea
¹⁷Department of Physics, Sejong University, Seoul, Republic of Korea
¹⁸Department of Physics, University of California, Berkeley, California, USA
¹⁹Department of Physics, University of Oslo, Oslo, Norway
²⁰Department of Physics and Technology, University of Bergen, Bergen, Norway
²¹Dipartimento di Fisica, Università di Pavia, Pavia, Italy
²²Dipartimento di Fisica dell'Università and Sezione INFN, Cagliari, Italy
²³Dipartimento di Fisica dell'Università and Sezione INFN, Trieste, Italy
²⁴Dipartimento di Fisica dell'Università and Sezione INFN, Turin, Italy
²⁵Dipartimento di Fisica e Astronomia dell'Università and Sezione INFN, Bologna, Italy
²⁶Dipartimento di Fisica e Astronomia dell'Università and Sezione INFN, Catania, Italy
²⁷Dipartimento di Fisica e Astronomia dell'Università and Sezione INFN, Padova, Italy
²⁸Dipartimento di Fisica 'E.R. Caianiello' dell'Università and Gruppo Collegato INFN, Salerno, Italy
²⁹Dipartimento DISAT del Politecnico and Sezione INFN, Turin, Italy
³⁰Dipartimento di Scienze MIFT, Università di Messina, Messina, Italy
³¹Dipartimento Interateneo di Fisica 'M. Merlin' and Sezione INFN, Bari, Italy
³²European Organization for Nuclear Research (CERN), Geneva, Switzerland
³³Faculty of Electrical Engineering, Mechanical Engineering and Naval Architecture, University of Split, Split, Croatia
³⁴Faculty of Engineering and Science, Western Norway University of Applied Sciences, Bergen, Norway
³⁵Faculty of Nuclear Sciences and Physical Engineering, Czech Technical University in Prague, Prague, Czech
³⁶Faculty of Physics, Sofia University, Sofia, Bulgaria
³⁷Faculty of Science, P.J. Šafárik University, Slovak Republic
³⁸Frankfurt Institute for Advanced Studies, Johann Wolfgang Goethe-Universität Frankfurt, Frankfurt, Germany
³⁹Fudan University, Shanghai, China
⁴⁰Gangneung-Wonju National University, Gangneung, Republic of Korea
⁴¹Gauhati University, Department of Physics, Guwahati, India
⁴²Helmholtz-Institut für Strahlen- und Kernphysik, Rheinische Friedrich-Wilhelms-Universität Bonn, Bonn, Germany
⁴³Helsinki Institute of Physics (HIP), Helsinki, Finland
⁴⁴High Energy Physics Group, Universidad Autónoma de Puebla, Puebla, Mexico
⁴⁵Horia Hulubei National Institute of Physics and Nuclear Engineering, Bucharest, Romania
⁴⁶HUN-REN Wigner Research Centre for Physics, Budapest, Hungary
⁴⁷Indian Institute of Technology Bombay (IIT), Mumbai, India
⁴⁸Indian Institute of Technology Indore, Indore, India
⁴⁹INFN, Laboratori Nazionali di Frascati, Frascati, Ital
⁵⁰INFN, Sezione di Bari, Bari, Italy
⁵¹INFN, Sezione di Bologna, Bologna, Italy
⁵²INFN, Sezione di Cagliari, Cagliari, Italy
⁵³INFN, Sezione di Catania, Catania, Italy

- ⁵⁴*INFN, Sezione di Padova, Padova, Italy*
⁵⁵*INFN, Sezione di Pavia, Pavia, Italy*
⁵⁶*INFN, Sezione di Torino, Turin, Italy*
⁵⁷*INFN, Sezione di Trieste, Trieste, Italy*
⁵⁸*Inha University, Incheon, Republic of Korea*
⁵⁹*Institute for Gravitational and Subatomic Physics (GRASP), Utrecht University/Nikhef, Utrecht, Netherlands*
⁶⁰*Institute of Experimental Physics, Slovak Academy of Sciences, Košice, Slovak Republic*
⁶¹*Institute of Physics, Homi Bhabha National Institute, Bhubaneswar, India*
⁶²*Institute of Physics of the Czech Academy of Sciences, Prague, Czech Republic*
⁶³*Institute of Space Science (ISS), Bucharest, Romania*
⁶⁴*Institut für Kernphysik, Johann Wolfgang Goethe-Universität Frankfurt, Frankfurt, Germany*
⁶⁵*Instituto de Ciencias Nucleares, Universidad Nacional Autónoma de México, Mexico City, Mexico*
⁶⁶*Instituto de Física, Universidade Federal do Rio Grande do Sul (UFRGS), Porto Alegre, Brazil*
⁶⁷*Instituto de Física, Universidad Nacional Autónoma de México, Mexico City, Mexico*
⁶⁸*iThemba LABS, National Research Foundation, Somerset West, South Africa*
⁶⁹*Jeonbuk National University, Jeonju, Republic of Korea*
⁷⁰*Johann-Wolfgang-Goethe Universität Frankfurt Institut für Informatik, Fachbereich Informatik und Mathematik, Frankfurt, Germany*
⁷¹*Korea Institute of Science and Technology Information, Daejeon, Republic of Korea*
⁷²*KTO Karatay University, Konya, Turkey*
⁷³*Laboratoire de Physique Subatomique et de Cosmologie, Université Grenoble-Alpes, CNRS-IN2P3, Grenoble, France*
⁷⁴*Lawrence Berkeley National Laboratory, Berkeley, California, USA*
⁷⁵*Lund University Department of Physics, Division of Particle Physics, Lund, Sweden*
⁷⁶*Nagasaki Institute of Applied Science, Nagasaki, Japan*
⁷⁷*Nara Women's University (NWU), Nara, Japan*
⁷⁸*National and Kapodistrian University of Athens, School of Science, Department of Physics, Athens, Greece*
⁷⁹*National Centre for Nuclear Research, Warsaw, Poland*
⁸⁰*National Institute of Science Education and Research, Homi Bhabha National Institute, Jatni, India*
⁸¹*National Nuclear Research Center, Baku, Azerbaijan*
⁸²*National Research and Innovation Agency - BRIN, Jakarta, Indonesia*
⁸³*Niels Bohr Institute, University of Copenhagen, Copenhagen, Denmark*
⁸⁴*Nikhef, National institute for subatomic physics, Amsterdam, Netherlands*
⁸⁵*Nuclear Physics Group, STFC Daresbury Laboratory, Daresbury, United Kingdom*
⁸⁶*Nuclear Physics Institute of the Czech Academy of Sciences, Husinec-Řež, Czech Republic*
⁸⁷*Oak Ridge National Laboratory, Oak Ridge, Tennessee, USA*
⁸⁸*Ohio State University, Columbus, Ohio, USA*
⁸⁹*Physics department, Faculty of science, University of Zagreb, Zagreb, Croatia*
⁹⁰*Physics Department, Panjab University, Chandigarh, India*
⁹¹*Physics Department, University of Jammu, Jammu, India*
⁹²*Physics Program and International Institute for Sustainability with Knotted Chiral Meta Matter (SKCM2), Hiroshima University, Hiroshima, Japan*
⁹³*Physikalisches Institut, Eberhard-Karls-Universität Tübingen, Tübingen, Germany*
⁹⁴*Physikalisches Institut, Ruprecht-Karls-Universität Heidelberg, Heidelberg, Germany*
⁹⁵*Physik Department, Technische Universität München, Munich, Germany*
⁹⁶*Politecnico di Bari and Sezione INFN, Bari, Italy*
⁹⁷*Research Division and ExtreMe Matter Institute EMMI, GSI Helmholtzzentrum für Schwerionenforschung GmbH, Darmstadt, Germany*
⁹⁸*Saga University, Saga, Japan*
⁹⁹*Saha Institute of Nuclear Physics, Homi Bhabha National Institute, Kolkata, India*
¹⁰⁰*School of Physics and Astronomy, University of Birmingham, Birmingham, United Kingdom*
¹⁰¹*Sección Física, Departamento de Ciencias, Pontificia Universidad Católica del Perú, Lima, Peru*
¹⁰²*Stefan Meyer Institut für Subatomare Physik (SMI), Vienna, Austria*
¹⁰³*SUBATECH, IMT Atlantique, Nantes Université, CNRS-IN2P3, Nantes, France*
¹⁰⁴*Sungkyunkwan University, Suwon City, Republic of Korea*
¹⁰⁵*Suranaree University of Technology, Nakhon Ratchasima, Thailand*
¹⁰⁶*Technical University of Košice, Košice, Slovak Republic*
¹⁰⁷*The Henryk Niewodniczanski Institute of Nuclear Physics, Polish Academy of Sciences, Cracow, Poland*
¹⁰⁸*The University of Texas at Austin, Austin, Texas, USA*
¹⁰⁹*Universidad Autónoma de Sinaloa, Culiacan, Mexico*
¹¹⁰*Universidade de São Paulo (USP), Sao Paulo, Brazil*
¹¹¹*Universidade Estadual de Campinas (UNICAMP), Campinas, Brazil*

- ¹¹²*Universidade Federal do ABC, Santo Andre, Brazil*
- ¹¹³*Universitatea Nationala de Stiinta si Tehnologie Politehnica Bucuresti, Bucharest, Romania*
- ¹¹⁴*University of Cape Town, Cape Town, South Africa*
- ¹¹⁵*University of Derby, Derby, United Kingdom*
- ¹¹⁶*University of Houston, Houston, Texas, USA*
- ¹¹⁷*University of Jyväskylä, Jyväskylä, Finland*
- ¹¹⁸*University of Kansas, Lawrence, Kansas, USA*
- ¹¹⁹*University of Liverpool, Liverpool, United Kingdom*
- ¹²⁰*University of Science and Technology of China, Hefei, China*
- ¹²¹*University of South-Eastern Norway, Kongsberg, Norway*
- ¹²²*University of Tennessee, Knoxville, Tennessee, USA*
- ¹²³*University of the Witwatersrand, Johannesburg, South Africa*
- ¹²⁴*University of Tokyo, Tokyo, Japan*
- ¹²⁵*University of Tsukuba, Tsukuba, Japan*
- ¹²⁶*Universität Münster, Institut für Kernphysik, Munster, Germany*
- ¹²⁷*Université Clermont Auvergne, CNRS/IN2P3, LPC, Clermont-Ferrand, France*
- ¹²⁸*Université de Lyon, CNRS/IN2P3, Institut de Physique des 2 Infinis de Lyon, Lyon, France*
- ¹²⁹*Université de Strasbourg, CNRS, IPHC UMR 7178, F-67000 Strasbourg, France, Strasbourg, France*
- ¹³⁰*Université Paris-Saclay, Centre d'Etudes de Saclay (CEA), IRFU, Département de Physique Nucléaire (DPHN), Saclay, France*
- ¹³¹*Université Paris-Saclay, CNRS/IN2P3, IJCLab, Orsay, France*
- ¹³²*Università degli Studi di Foggia, Foggia, Italy*
- ¹³³*Università del Piemonte Orientale, Vercelli, Italy*
- ¹³⁴*Università di Brescia, Brescia, Italy*
- ¹³⁵*Variable Energy Cyclotron Centre, Homi Bhabha National Institute, Kolkata, India*
- ¹³⁶*Warsaw University of Technology, Warsaw, Poland*
- ¹³⁷*Wayne State University, Detroit, Michigan, USA*
- ¹³⁸*Yale University, New Haven, Connecticut, USA*
- ¹³⁹*Yonsei University, Seoul, Republic of Korea*
- ¹⁴⁰*Zentrum für Technologie und Transfer (ZTT), Worms, Germany*
- ¹⁴¹*Affiliated with an institute covered by a cooperation agreement with CERN*
- ¹⁴²*Affiliated with an international laboratory covered by a cooperation agreement with CERN*

^aDeceased.

^bAlso at Max-Planck-Institut für Physik, Munich, Germany.

^cAlso at Italian National Agency for New Technologies, Energy and Sustainable Economic Development (ENEA), Bologna, Italy.

^dAlso at Dipartimento DET del Politecnico di Torino, Turin, Italy.

^eAlso at Yıldız Technical University, Istanbul, Türkiye.

^fAlso at An institution covered by a cooperation agreement with CERN.

^gAlso at Department of Applied Physics, Aligarh Muslim University, Aligarh, India.

^hAlso at Institute of Theoretical Physics, University of Wrocław, Poland.